PROCEEDINGS, Twentieth Workshop on Geothermal Reservoir Engineering
Stanford University, Stanford, California, January 24-26 1995
SGP-TR-150

Effect of Sorption/Curved Interface Thermodynamics on Pressure transient

K.T.Lim and K.Aziz
Stanford University

January 1995

Abstract

A simulation model capable of handling the effects of sorption was constructed. It accounts for the curved interface thermodynamics associated with adsorption and desorption. Data from several laboratory experiments were used to verify the model. The results indicated that simulation runs using sorption isotherms adequately model the pressure transient behavior observed in the laboratory experiments. Dry steam models severely underestimated the the effective compressibility. Models using flat-interface (steam table) thermodynamics over-estimated the compressibility of the system, indicated by slower than actual rate of pressure transient propagation.

1 Introduction

In a porous medium, the interface between different fluid phases is seldom flat, like the one that would occur when the fluid is placed in a large container. The phase occurring on the concave side of a curved interface can exist at a pressure lower than its corresponding saturation pressure. (Saturation pressure is defined as the equilibrium pressure with a flat interface.) For a vapor-liquid system in equilibrium this phenomenon explains the existence of the vapor phases at pressures lower than the saturation pressure, commonly known as the vapor pressure lowering effect. Other thermodynamic effects due to the presence of a curved interface are discussed in Section 2.

The objective of this work is to construct a numerical model that honors the thermodynamics of sorption in the presence of curved interfaces. This was achieved by treating laboratory measured sorption isotherms as the governing mass balance relationship, and accounting for the thermodynamic effects of curved interfaces in the mass and energy balance equations. The model also has a separate option of using flat-interface (steam table) thermodynamics for comparison. The flat-interface option of the simulator has been verified by successfully modeling all of the cases in the Stanford Geothermal Model Intercomparison Study (1980). The numerical model with sorption was verified by modeling various laboratory adsorption and desorption experiments. Comparisons were made against models with flat-interface thermodynamics and single-phase dry steam. The following discussions focus on the implementation of the sorption model.

2 Thermodynamic Effects of Curved Interface

Apart from the vapor-pressure lowering effect, the presence of a curved interface also causes an increase in the heat of vaporization compared to that with a flat interface. Equilibrium thermodynamics analyses also showed that curved interface causes both phases to exist in superheated states (Udell 1982). The thermodynamics relationships outlined in this section follow those of Defay and Prigogine (1966) and Kaviany (1991).

2.1 Vapor Pressure Lowering

Consider a liquid and a vapor phase in equilibrium in the presence of a curved interface. Starting with the Gibbs-Duhem equation for each phase, it can be shown that the presence of a curved interface implies the existence of a pressure difference between the liquid and vapor phases — the capillary pressure:

$$p_c = p_v - p_l \quad (1)$$

The phase occurring on the concave side of a curved interface can exist in equilibrium at a pressure lower than its corresponding saturation pressure by a quantity equal to the capillary pressure.

2.2 Liquid Superheat

The thermodynamics relationship for determining the amount of superheat in the liquid phase is:

$$\left(\frac{1}{T} - \frac{1}{T^o}\right) = \frac{R}{h_{fg}} \ln\left(\frac{p_v}{p_l}\right) \qquad (2)$$

The quantity $(T-T^o)$ is the degree of superheat in the liquid phase. By honoring Eq. 2 while solving for p_l as a secondary variable an input of p_c is unnecessary because it will overconstrain the solution.

2.3 Increase in Heat of Vaporization

The presence of curvature also causes an increase in the heat of vaporization in comparison with the corresponding value when a flat interface is present:

$$h_{fg} = h^\circ_{fg} + \left(v_l - T\left.\frac{\partial v_l}{\partial T}\right|_{p_l}\right)(p_c) \qquad (3)$$

where the superscript '°' refers to a case with flat-interface. In general (Kaviany, 1991),

$$v_l \gg T\left.\frac{\partial v_l}{\partial T}\right|_{p_l}$$

so that the last term in Eq. 3 can be ignored. In the model the heat of vaporization is computed as:

$$h_{fg} = h^\circ_{fg} + \left(\frac{p_v - p_l}{\rho_l}\right) \qquad (4)$$

3 Governing Equations

Mass, energy and momentum balances are the three governing equations of fluid flow. For a given component c in a multicomponent system the mass balance equation is:

$$\frac{\partial}{\partial t}\left[\sum_p y_{cp}\phi\rho_p S_p\right] + q^w_c - \sum_p \nabla\cdot[y_{cp}\rho_p\vec{v}_p] = 0 \qquad (5)$$

The terms in Eq. 5 are, respectively, rate of accumulation, source/sink term and net influx of component c. For a given phase p, the momentum balance in a porous media is governed by Darcy's Law:

$$\vec{v}_p = \frac{kk_{rp}}{\mu_p}(\nabla p_p - \rho_p\, g\nabla D) \qquad (6)$$

Eqs. 5 and 6 are combined to form a mass balance equation for each component.
The energy balance equation is:

$$\frac{\partial}{\partial t}\left[\sum_p \phi\rho_p S_p U_p + (1-\phi)\rho_r U_r\right] + q^w h^w - H$$

$$-\sum_p \nabla\cdot(\rho_p\vec{v}_p h_p) - \nabla\cdot(\lambda\nabla T) = 0 \qquad (7)$$

The physical meaning of the terms in Eq. 7 are, respectively, rate of accumulation of internal energy, heat production, specified heat influx, energy associated with fluid influx and heat conduction term.

3.1 Primary Variables

Each simulation gridblock has n_c mass balance equations and one energy balance equation. Therefore, the number of independent primary variables required is $n_c + 1$. The primary variables are chosen such that the variables are independent of one another over all physical regions of the fluid system. The primary variables chosen for this study are

- p_v (pressure in the vapor phase, 1 variable)
- z_c (overall mole fractions of component c, $n_c - 1$ variables)
- h (overall specific enthalpy of fluid, 1 variable)

For a single component system, the primary variables are p_v and h.

3.2 Secondary Variables

After the primary variables are obtained, the remaining variables can be determined using constitutive relationships and phase equilibrium calculations. The variables to be determined are temperature, liquid phase pressure and phase saturations. Flat-surface thermodynamics and regions with sorption (i.e. curved interface) are treated separately. The following discussion is limited to single component, two-phase systems.

3.2.1 Flat-Interface Thermodynamics

A flat interface between the liquid and vapor phases implies that both phases exist at the same pressure. Saturated steam (steam table) properties are applicable.

In the two phase region pressure and temperature are dependent on each other, and saturations can be easily determined from the primary unknowns. At a given temperature, mass transfer between the phases can occur without a change in pressure.

In the single phase (compressed water and superheated steam) regions fluid properties are functions of both pressure and temperature. The temperature is determined iteratively by satisfying all constitutive relations and equilibrium thermodynamics. Convergence can be easily obtained in very few iterations because the temperature of a reservoir does not vary much, with the probable exception around source or sink locations.

3.2.2 Sorption

In the sorption model the mass balance is influenced by the sorption isotherm. The isotherms relate the mass adsorbed to pressure and specified temperatures. Knowledge of the pressure and temperature would allow explicit determination of phase saturations. To account for temperature variations, mass-relative pressure isotherms are internally converted to mass-activity relationships (Hsieh and Ramey, 1983). For a given adsorbed mass (X, mass-of-water/mass-of-rock) the liquid saturation is:

$$S_l = \frac{1-\phi}{\phi} \frac{\rho_r}{\rho_l} X \qquad (8)$$

In this case the liquid phase pressure, p_l, becomes a secondary unknown instead of saturation. It is to be determined by satisfying all the thermodynamic effects described in section 2.

4 Verification

Results from three separate sets of laboratory pressure transient experiments were used to verify the numerical models. All numerical models are one-dimensional. Analyses were made for the case of a single component steam-water system. For comparison purposes, the corresponding cases assuming flat-interface thermodynamics and dry steam were also analyzed. The flat surface thermodynamics cases were initialized with the same liquid saturations as those in the corresponding cases with sorption. The dry-steam cases assumed zero liquid saturation and that the steam remained as single phase vapor at all times.

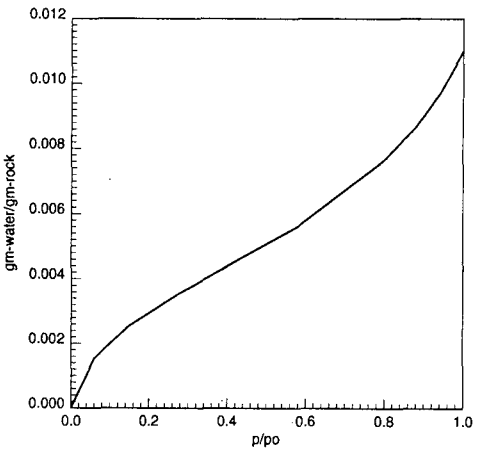

Figure 1: Isotherm for temperature of 146°C, from Herkelrath et al. (1983).

Analyses also showed that the results were not sensitive to the gridblock sizes, but are very sensitive to the sorption isotherms.

4.1 Adsorption: Data of Herkelrath et al. (1983)

Herkelrath et al. (1983) conducted a series experiments to study the transient steam flow in a uniform porous medium. A sample holder 61 cm long with an internal diameter of 5.04 cm was used. Transient, superheated steam flow experiments were run by first bringing the porous material to a uniform initial pressure. A step increase in pressure was imposed at one end of the sample by exposing it to a saturated steam reservoir while measuring the pressure at the other end. The experiments were conducted at 100°, 125° and 146°C. The corresponding adsorption isotherm was measured separately. Fig. 1 shows the isotherm for this study.

Laboratory data and simulation results for the experiment conducted at 146°C are shown in Fig. 2. Simulation results assuming gas flow theory (for the case labeled dry steam) and flat interface thermodynamics are also shown. The results showed that the transient pressure response could be adequately modeled with the sorption model using the measured adsorption isotherm. This observation was also made by Herkelrath et al. (1983). The sorption model takes

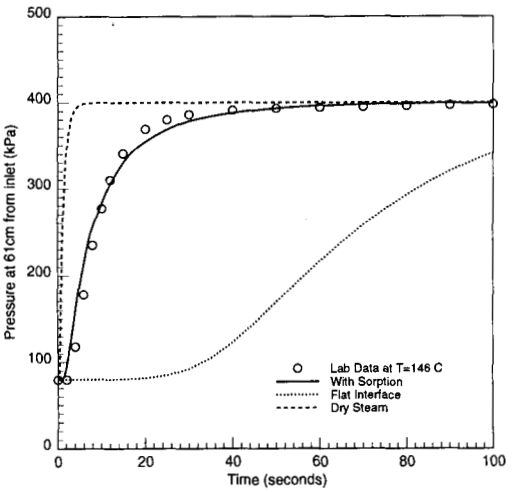

Figure 2: Transient flow experiment of Herkelrath et al. (1983) at 146°C.

into account the fact that there always exists a pressure difference between the vapor and liquid phases and can be adequately represented by the pressure-sorption relationship contained in the isotherm. The dry steam case severely underestimated the time required for the pressure at one end of the core to reach the pressure imposed at the other end. This is due to the absence of phase change associated with adsorption of steam on the rock surfaces, which would reduce the speed of pressure propagation. Assuming flat surface thermodynamics, on the other hand, caused a delay in pressure response compared to the experimental data. This is because the quantity $\frac{\partial V}{\partial p}$ at a given temperature is infinite in the two phase region. In each simulation gridblock this phenomenon results in steam condensation at an almost constant pressure. Pressure changed during condensation because the model was not isothermal, with the injected steam having a higher temperature than the initial conditions in the model. The is reflected in the simulation result as a model having very large apparent compressibility.

To illustrate the differences in pressure responses, the pressure distributions at various times for the sorption and flat-interface models are shown in Figs. 3 and 4, respectively. With flat surface thermodynamics, the speed of pressure propagation is almost an order of magnitude slower compared to that with sorption. Pressure distributions at 1 and 5 second for the sorption model resembles those at 10 and 50 seconds for the flat interface model.

Results of the 100° and 125°C cases showed essentially the same results as the 146°C case.

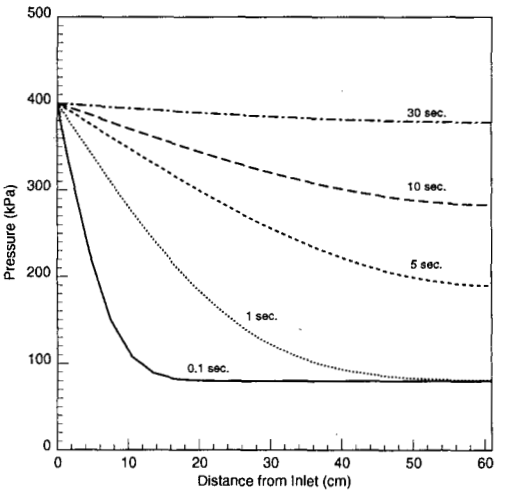

Figure 3: Pressure distributions for the 146°C case, sorption model.

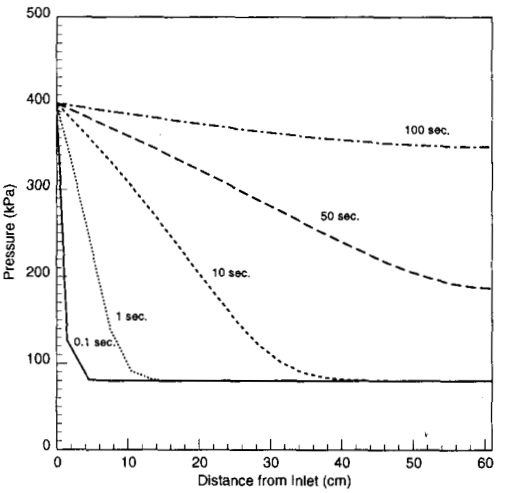

Figure 4: Pressure distributions for the 146°C case, with flat-interface thermodynamics.

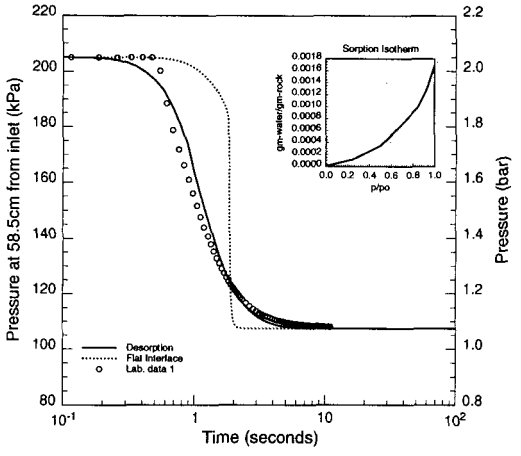

Figure 5: Desorption experiment of Palar and Horne (1994).

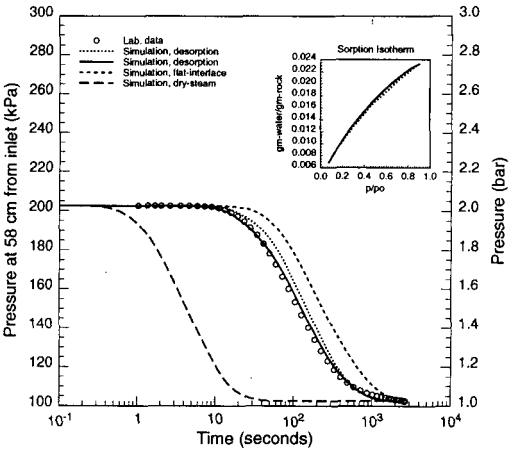

Figure 6: Desorption experiment of Herkelrath (1994)

4.2 Desorption: Data of Palar and Horne (1994)

Palar and Horne (1994) used equipments similar to that of Herkelrath et al. (1983) to conduct desorption experiments. A rock sample from the Geysers geothermal field was used. The sample was exposed to saturated steam at about 125°C and the corresponding saturation pressure. One end of the sample holder was exposed to the atmosphere while the pressure change at the other end was monitored. Fig. 5 shows the measured transient pressure decline against time. Due to the low level of adsorption (the estimated overall liquid saturation is less than 1 per cent), and high permeability of the sample (37.5 darcy) the pressure decline propagated to the closed end of the sample holder very rapidly. Also shown in Fig 5 are the simulated results with the sorption and flat-interface models. The sorption isotherm inset in Fig 5 is the isotherm used in the simulation model. The isotherm is a slight modification of that obtained by Palar and Horne (1994) using regression analysis. Again the sorption model gives a good match with the laboratory observations. The flat-interface model results implied a very large effective compressibility, as indicated by the delayed pressure drop.

4.3 Desorption: Data of Herkelrath (1994)

The experiment was run using a column packed with Tipperary Sand, a dune sand obtained near Fallon, Nevada. The samples contain only the less-than 106 micron fraction of the sand. The following are the sample data:

sample mass	1941 g
sample length	58 cm
sample diameter	5.2 cm
porosity	0.42
permeability	1.61E-08 cm**2

Steam pressure-drawdown experiment was run at 123°C. The sample was evacuated and then charged with steam until the steam pressure reached 2.026 bars, and the temperature stabilized. At time=0, the bottom of the sample was opened to the atmosphere, and the pressure at the top of the sample was monitored as a function of time. Sorption isotherm was measured in a separate equilibrium experiment using the same sample. Simulation results are shown in Fig. 6. The dotted line is the results obtained using sorption data of Herkelrath (1994). It gave a much better match to the laboratory data than either the dry-steam or the flat-interface case. An excellent match was obtained by modifying the sorption isotherm very slightly, as shown by the solid line in Fig. 6. Considering the fact that the same sample was used for two separate experiments with different packings, the differences between the isotherms shown in Fig. 6 are well within experimental accuracy.

5 Conclusions

From the preceding discussions the following conclusions can be made:

1. A numerical model capable of honoring the thermodynamics of sorption has been constructed and verified against laboratory experiments.
2. Pressure transient due to sorption could be adequately modeled using equilibrium sorption isotherms, and the results were in excellent agreement with experimental observations.
3. Sorption of steam on rock surfaces results in delayed transient pressure response and in a higher apparent compressibility compared to a dry steam case. However, the apparent compressibility due to sorption is much lower than that of a flat-interface model.
4. Direct application of steam table properties in the flat interface models resulted in very large apparent compressibilities and in delayed pressure transient propagation compared to those observed in experiments.

Nomenclature

h = specific enthalpy
H = heat influx
k = permeability
k_r = relative permeability
p = pressure
p_c = capillary pressure
R = universal gas constant
T = temperature
q = source/sink term
s = specific enthropy
S = saturation
t = time
T = temperature
U = specific internal energy
v = specific volume
$\vec{v}$ = velocity
X = adsorption, mass/mass-of-rock
y = mole fraction
z = overall mole fraction
λ = thermal conductivity
μ = viscosity, or chemical potential
ϕ = porosity
ρ = density

Subscripts

c = component
g = gas phase
l = liquid phase
r = rock
p = a given phase
v = vapor phase

Superscripts

$^\circ$ = saturated state
^{T} = total
^{w} = well

References

[1] Defay, R. and Prigogine, I.: *Surface Tension and Adsorption*, J. Wiley (1966).

[2] Herkelrath, W.N., Moench, A.F. and O'Neal, C.F. II.: "Laboratory Investigation of Steam Flow in a Porous Medium," *Water Resources Research, Vol* 19, No. 4, August 1983, 931-37.

[3] Herkelrath, W.N., personal communication, June 1994.

[4] Hsieh, C.H. and Ramey, H.J. Jr.: "Vapor-Pressure Lowering in Geothermal Systems," *SPEJ*, February 1983, 157-67.

[5] Kaviani, M.: *Principles of Heat Transfer in Porous Media*, Springer-Verlag (1991).

[6] Palar, S. and Horne, R.N.: "The Effect of CO_2 on Steam Adsorption," presented at the 19th Stanford Geothermal Workshop, Stanford CA., Jan. 18-20, 1994.

[7] Stanford Geothermal Program TR-42: "Proceedings, Special Panel on Geothermal Model Intercomparison Study," Stanford, CA., December 1980.

[8] Udell, K.S.: "The Thermodynamics of Evaporation and Condensation in Porous Media," SPE 10779 presented at the 1982 California Regional Meeting of SPE, San Francisco, CA., March 24-26, 1982.